Chapter 5

Thick-Film Resistor Failure Analysis Based on Low-Frequency Noise Measurements

Ivanka Stanimirović

Additional information is available at the end of the chapter

http://dx.doi.org/10.5772/intechopen.69442

Abstract

The chapter aims to present research results in the field of thick-film resistor failure analysis based on standard resistance and low-frequency noise measurements. Noise spectroscopy–based analysis establishes correlation between noise parameters and parameters of noise sources in these heterogeneous nanostructures. Validity of the presented model is verified experimentally for resistors operating under extreme working conditions. For the experimental purposes, thick-film resistors of different sheet resistances and geometries, realized using commercially available thick-film resistor compositions, were subjected to high-voltage pulse (HVP) stressing. The obtained experimental results are qualitatively analysed from microstructure, charge transport mechanism and low-frequency noise aspects. Correlation between resistance and low-frequency noise changes with resistor degradation and failure due to high-voltage pulse stressing is observed.

Keywords: thick-film resistors, low-frequency noise, conducting mechanisms, high-voltage pulse stressing, failure analysis

1. Introduction

Thick-film technology that has been in continuous use for decades, mostly in commercial and specialized electronics, is once again increasing interest. The revival of thick-film technology can be attributed to the increasing application of ceramic micro-electro-mechanical systems (C-MEMSs) and the communications industry's need for electronic circuitry with increased functional capability, reduced weight, improved reliability and environmental stability. When C-MEMS are in question, thick-film technology provides simultaneous realization of sensor and actuator elements as well as electronic circuitry for signal processing. In addition, thick-film resistors, the key assets of thick-film technology, are being used both as sensing and as

resistive elements. This new application of thick-film resistive materials leads to reduction in resistor dimensions, higher required tolerances and increasing use of buried components. On the other hand, increasing application of thick-film devices in communication systems requires better knowledge of their modulation effects in these systems that are correlated to low-frequency noise sources in thick resistive films. Since noise investigations are powerful tools in reliability investigations it is of the great importance to determine whether standard low-frequency noise measurements can be used in evaluation of these complex structures. Low-frequency noise in thick-film resistors depends on their microstructure and for that reason it can be used to track structural changes caused by different types of stressing conditions that affect reliability of the film. Relationship between low-frequency noise and structure of thick resistive films has mostly been investigated experimentally. The theoretical problem is not simple because of the thick-film's quite complex microstructure. The variety of the parameters that has to be taken into consideration is certainly one of the most significant limitations. However, data related to thick-film compositions and technological processes can provide information about ranges of parameter values. Moreover, the formation of conducting paths and metal-insulator-metal (MIM) units requires the special attention. For these reasons, this chapter focuses on the correlation between noise parameters and parameters of noise sources in thick-film resistors. Firstly, a model of low-frequency noise in thick resistive films that relate noise parameters to thick-film structural and electrical characteristics is described. Then, failure analysis of thick-film resistors subjected to high-voltage pulse stressing is presented based on resistance and low-frequency noise measurements. At the closing subsection, the brief summary of the topic is presented with an emphasis on the possibility that standard resistance and noise measurements can be used in degradation and failure analysis of thick resistive structures under a wide range of extreme working conditions.

2. Low-frequency noise in thick-film resistive structures

Transport of electrical charges in thick-film materials takes place via chains of conducting particles (**Figure 1**) [1]. Two adjacent conducting particles in the chain can be sintered or insulated by a thin, glass barrier thus determining the electrical current flow. Therefore, metallic conduction and direct tunnelling are dominant conducting mechanisms present in thick resistive films. Tunnelling via traps is also present in thick-film resistors but it is a dominant conducting mechanism when thick insulating layers are in question. Since the insulator layers are thin [2], direct tunnelling is one of the dominant conduction mechanisms [3]. For low applied voltages $V_B \gg \Phi_B$, where Φ_B is the height of the potential barrier, the applied voltage and the current are proportional. Resistance of the resistor is determined by the barrier resistance. Trap at the location x_1, shown in **Figure 1**, is being randomly occupied by electron. Therefore, its presence modulates the direct tunnelling current. Because of the barrier height, field and thermal injection effects are neglected.

Low-frequency noise sources in these noisy devices are correlated to following conducting mechanisms:

http://dx.doi.org/10.5772/intechopen.69442

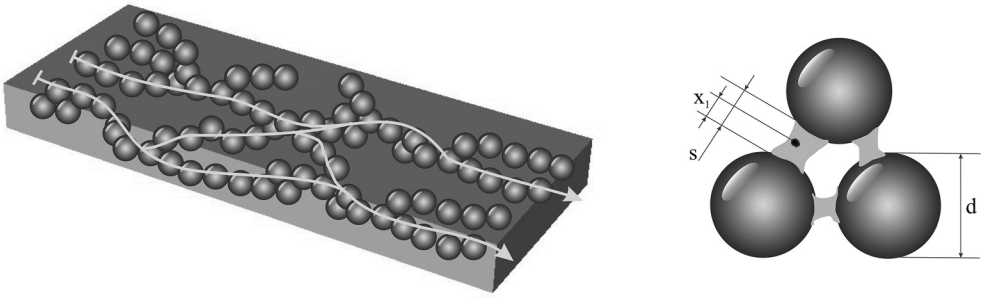

Figure 1. Schematic presentation of thick-film resistor and a segment of a chain where adjacent conducting particles are separated by thin insulating layers.

1. Metallic conduction

Hooge's empirical expression [4] describes low-frequency relative voltage noise spectrum for conduction through conductive grains and contacts between them:

$$\frac{S_{\mathrm{VC}}}{V_{\mathrm{C}}^2} = \frac{\alpha}{V_{\mathrm{ef}} n f}, \tag{1}$$

where α is the Hooge numerical parameter of the order of 10^{-3}, while V_{ef} and n are the effective volume of sintered contact and free carriers concentration in the contact region, respectively. Hooge's expression is used as the empirical relation with the effective parameters in order to express $1/f$ noise, which is a consequence of contact and particle resistivity fluctuations.

2. Tunnelling processes

When conduction through glass barriers is in question, low-frequency fluctuations of tunnelling processes are correlated to the glass matrix space charge fluctuations. These fluctuations can be caused by the presence of traps in glass barriers and fluctuations caused by the thermal noise in the glass matrix [5]. If it is assumed that potential barrier height fluctuations are caused by Nyquist noise of the insulator, then the relative voltage noise spectrum due to the Nyquist noise modulation can be given by the following expression [1, 5]:

$$\frac{S_{\mathrm{VBN}}}{V_B^2} = \frac{4\pi m q k T}{3\Phi_B h^2} \cdot tg\delta \cdot \frac{s^2}{C} \cdot \frac{1}{f}, \tag{2}$$

where q and m are the electron charge and its effective mass, h is the Planck's constant, k is the Boltzmann's constant, T is the absolute temperature, s is the thickness of the insulating layer, $tg\delta$ is the loss tangent of the insulator, Φ_B is the potential barrier height measured with respect to the Fermi energy and C is the capacitance of metal-insulator-metal (MIM)

unit [1] that consists of two spherical conducting particles separated by a thin insulating layer.

If it is assumed that MIM insulating layers contain traps, the trap may be of neutral or negative charge. The trap may have negative charge as a consequence of occupation by electron during the tunnelling process. The trap occupation function fluctuation induces the barrier height fluctuation due to the local charge fluctuation. In calculations of noise spectrum due to the trap occupation fluctuations, the following is taken into account:

i. the greatest contribution to the noise is the traps with energies equal to the Fermi level in the conducting particle,

ii. the potential barrier is rectangular and of height Φ_B and width s, and

iii. the applied voltage V_B is low, i.e. $V_B \gg \Phi_B$.

In that case, the relative voltage noise spectrum due to the presence of traps in glass barriers is given by the following expression [6, 7]:

$$\frac{S_{\mathrm{VB}}}{V_B^2} = \frac{8\pi m q^3 s^2 x_1^2 \chi}{h^2 A^2 \Phi_B \varepsilon_0^2 \varepsilon_r^2} \frac{\theta}{(1+\theta)^2} \frac{\tau}{1+\omega^2\tau^2}, \tag{3}$$

where x_1 is the position of the trap (**Figure 1**), A is the barrier cross-section, ε_0 is the vacuum electrical permittivity, ε_r is the relative electrical permittivity of the glass, while χ and θ are parameters given by the following expressions:

$$\chi = \left(1 - \frac{x_1}{s}\right)^2 \left[\left(1 - \frac{x_1}{s}\right)^2 + \frac{x_1^2}{s^2}\right], \tag{4}$$

$$\theta = \frac{\tau_c}{\tau_e}. \tag{5}$$

The reciprocal time parameter τ is defined as

$$\tau^{-1} = \tau_c^{-1} + \tau_e^{-1} = C_1 n(E) \exp\left(-2\int_0^{x_1} |k| dx\right) + C_2 \exp\left(-2\int_{x_1}^{s} |k| dx\right), \tag{6}$$

where $|k|$ is the electron wave vector magnitude. The concentration $n(E)$ is the free electron concentration in the conducting particle, with energy E equal to the Fermi energy E_{fm}. C_1 and C_2 are constants of electron capture and emission. The random occupation of the trap depends on the random tunnelling of the electron between two particles separated by a thin glass barrier that contains the trap. As the consequence of the presence of the single-energy level trap, Lorentzian terms may be present in low-frequency noise spectrum of the resistor. The distribution of the trap energy levels can result in noise spectrum with $1/f^{\gamma}$ dependence ($\gamma = 1$ or $\gamma \neq 1$) [8].

http://dx.doi.org/10.5772/intechopen.69442

Under assumption that thick-film resistor can be viewed as the complex network [1] that consists of M parallel chains and that one chain consists of K_C contacts and K_B MIM units, then the total resistance of the resistor is given by

$$R = \frac{K_C R_C + K_B R_B}{M^2}, \tag{7}$$

where R_C is the resistance of the sintered contact between two neighbouring conducting particles and R_B is the barrier resistance. Resistance of the sintered contact between two adjacent conducting particles is determined by the specific resistance of the contact ρ and the radius of the barrier cross section a [1]:

$$R_C = \frac{\rho}{\pi a}. \tag{8}$$

In the case of neighbouring particles separated by a thin glass barrier, resistance of the MIM unit is determined by the barrier resistance [1]:

$$R_B = \frac{h^2 s}{q^2 A (2mq\Phi_B)^{1/2}} \exp\left[\left(\frac{32\pi^2 mqs^2\Phi_B}{h^2}\right)^{1/2}\right]. \tag{9}$$

The tunnelling area A can be calculated as $A = \pi a^2$, where a is the radius of the area that depends on the diameter d of the conducting particle.

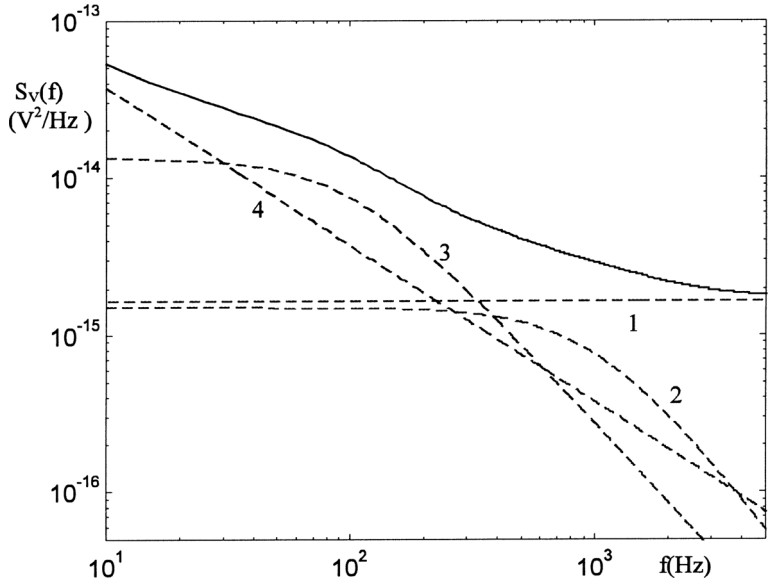

Figure 2. Contributions of different kinds of the noise sources in the total voltage noise spectrum (continuous line) as calculated using Eq. (10) (1—thermal noise; 2, 3—noise due to the presence of traps in glass barriers; and 4—1/*f* noise) [6].

The total relative voltage noise spectrum is therefore given by the following expression [6]:

$$\frac{S_V}{V^2} = \frac{1}{N_C} \frac{1}{\left(1 + \frac{N_B R_B}{N_C R_C}\right)^2} \frac{S_{VC}}{V_C^2} + \frac{1}{N_B} \frac{1}{\left(1 + \frac{N_C R_C}{N_B R_B}\right)^2} \left\{ \frac{S_{VBN}}{V_B^2} + \frac{S_{VB}}{V_B^2} \right\}. \tag{10}$$

where N_B, N_T and N_C are the total number of barriers, traps and contacts, respectively, taking part in the conduction process between two opposite electrodes.

Contributions of different kinds of noise sources included in Eq. (10) are shown in **Figure 2**. These results are obtained by numerical simulation for parameter values: $s = 1.33$ nm, $d = 150$ nm, $a = 6.2$ nm, $N_B = 3.8 \times 10^8$, $N_C = 4.6 \times 10^9$, $N_T = 6.9 \times 10^9$ and $R = 100$ kΩ [6]. $1/f$ noise and noise due to the presence of traps in glass barriers are included along with two Lorentzian terms ($f_{C1} =$ 115 Hz and $f_{C2} = 1.1$ kHz). The contribution of the noise due to the conduction through the conductive grains or contacts between the adjacent ones is negligible, and, therefore, is not shown in **Figure 2**.

3. Failure analysis of thick-film resistors subjected to high-voltage pulse stressing

Different conditions of thick-film resistor application have induced the need to investigate their behaviour under stress, especially high-voltage pulse stress. The most of the published data dealt with trimming of thick resistive films by energy of high-voltage pulses (HVP trimming) [9, 10]—a trimming method based on internal discharges using both thick-film resistor terminations as electrodes for applying the high-voltage energy to the resistor body. Moreover, several papers explored properties of thick-film surge resistors [11] that serve as protection of communication systems from a variety of voltage disturbances such as short duration, high-voltage transients caused by lightning strikes or longer duration over voltages. Nowadays, the revival of thick-film technology that can be attributed to new applications of thick-film resistors induced the necessity of extensive behavioural studies related to undesirable high-voltage pulse stressing of conventional thick resistive films [12–14].

In order to qualitatively analyse the influence of high-voltage pulsing on thick-film resistors, pulse performances have been investigated using a model of low-frequency noise in thick resistive films presented in the previous chapter. Behavioural analysis of thick-film resistors subjected to high-voltage pulse stressing was performed using several groups of thick-film test samples with different resistor geometries (**Figure 3**) realized using commercially available RuO_2 and $Bi_2Ru_2O_7$ mixture-based-thick-film resistor compositions in combination with Pd/Ag conductor composition. Test samples were formed on ceramic alumina (96% Al_2O_3) substrates using conventional screen-printing techniques. After 15 min levelling at 21°C, wet layers were dried at 150°C in a conveyer infrared drier for 10 min. Dry resistive films were 25 ± 3 μm thick. Firing was performed using standard 30-min cycle ($T_{max} = 850$°C, $t_{max} = 10$ min). Pulse performances have been investigated using 100/700 μs pulses delivered by Haefely P6T impulse tester

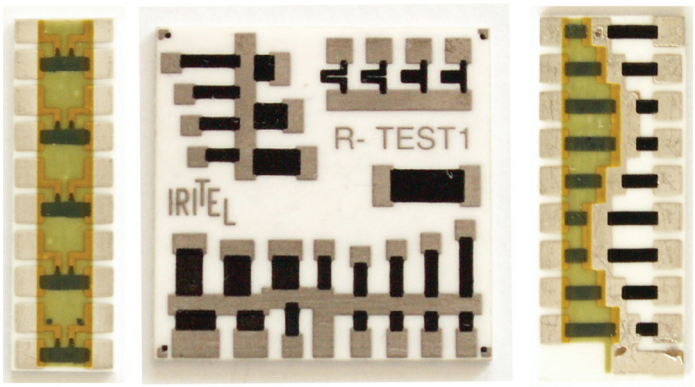

Figure 3. Thick-film test resistors of different lengths and widths used in experimental investigations.

with an output resistance of 25 Ω. Following experimental set-up was used: 1.5–4.0 kV voltage range, 10 pulse series, 6 pulses/min frequency, $T = 21°C$. Testing conditions were selected in compliance with ITU-T K.20 standard that refers to the resistibility of telecommunication equipment to over-voltages and over-currents. Keithley nanovolt amplifier, Model 103A, was used for voltage noise spectrum measurements along with Hewlett-Packard dynamic signal analyzer 3561B in the 10 Hz to 10 kHz frequency range. A noise index [15] was also measured in compliance with the test method standard for electronic and electrical component parts MIL-STD-202D, Method 308, at 1 kHz. For noise index measurements, Quan-Tech Resistor Noise Test Set, Model 315B was used. Hewlett-Packard 34401A instrument was used for resistance measurements.

Table 1 and **Figure 4** [12] present typical results obtained by noise and resistance measurements for 10 and 100 kΩ/sq test resistors that were exposed to the high-voltage treatment. Resistors with identical 1×2 mm^2 geometries suffered degradation but they did not catastrophically fail. Results obtained by noise index, voltage noise spectrum and resistance

Degradation			**Catastrophic failure**		
R_{sq} (kΩ/sq)	10	100	R_{sq}(kΩ/sq)	10	100
R_N (kΩ)	16	220	R_N (kΩ)	8	110
$\overline{R_i}$ (kΩ)	15.942	220.060	R_i (kΩ)	7.842	111.92
$\overline{R_s}$ (kΩ)	15.490	217.650	R_S (kΩ)	22.55	11.8(→105.5)
$\overline{S_{R_i}}$ (Ω^2/Hz)	2.508×10^{-7}	2.45×10^{-4}	S_{R_i}(Ω^2/Hz)	9.89×10^{-8}	2.48×10^{-4}
$\overline{S_{R_s}}$ (Ω^2/Hz)	5.2289×10^{-5}	2.4×10^{-3}	S_{R_s} (Ω^2/Hz)	1.5×10^{-2}	7.13×10^{-4}
$\overline{NI_i}$ (dB)	−23.8	−7.5	NI_i (dB)	−15.2	7
$\overline{NI_s}$ (dB)	−0.8	0.5	NI_s (dB)	21.7	24.2

Table 1. Resistor parameters before (i) and after (s) high-voltage pulse stressing [12].

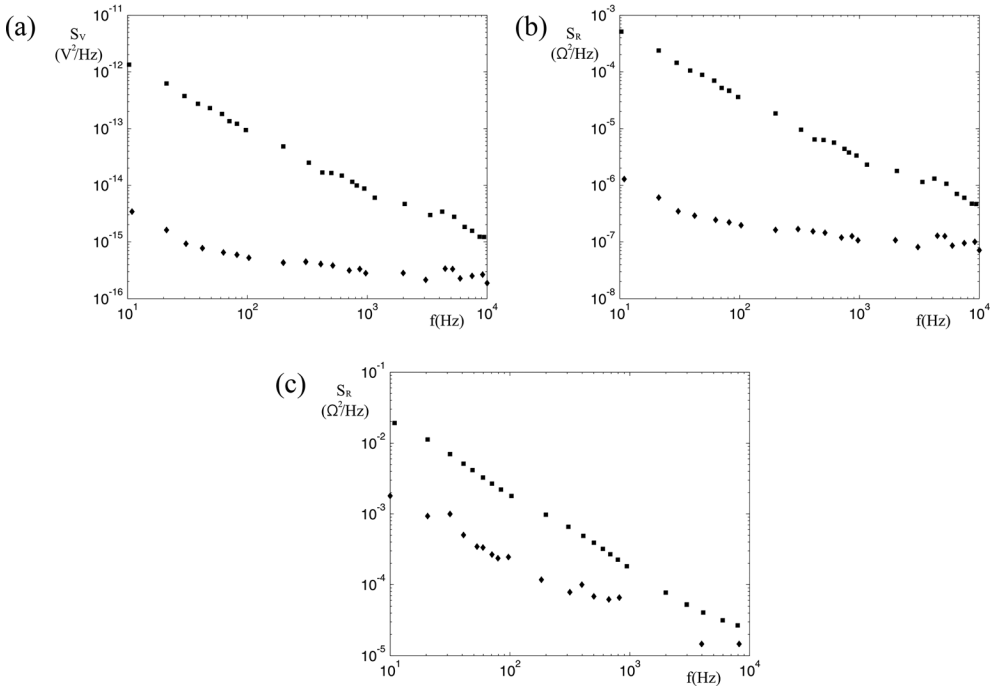

Figure 4. Experimental results for voltage and resistance noise spectra (◆—before pulse stressing, ■—after pulse stressing), for thick-film resistors with following nominal resistances: $R = 16$ kΩ (a, b) and $R = 220$ kΩ (c) [12].

measurements are given for resistors with a nominal resistance of 16 kΩ that were subjected to the impact of eleven 1500 V pulses and a single 3000 V pulse and resistors with a nominal resistance of 220 kΩ that were subjected to the impact of eleven 1500 V pulses and eleven 3000 V pulses. After impacts of the first and the tenth pulse from the series of pulses with the same amplitude, voltage noise spectrum and resistance measurements were performed. Results for two series of degraded resistors (10 and 100 kΩ/sq) and two resistors that suffered catastrophic failure are given in **Table 1**. Sheet resistances, R_{sq}, nominal resistances, R_N, resistances, R, resistance noise spectra, S_R, and noise indexes, NI, before (i) and after (s) high-voltage pulse treatment are presented.

Results given in **Table 1** show that resistance decreases with high-voltage pulse treatment of thick resistive films. The relative resistance change for both groups of resistors is of the order of several percents. This change although small is higher for 10 kΩ/sq resistors (3%) than for 100 kΩ/sq resistors (1%).

Figure 4 presents the experimental results for resistance noise spectra before and after high-voltage pulse stressing. Since the voltage noise spectrum depends on current I, the measured values for the voltage noise spectrum were used for resistance noise spectrum ($S_R = S_V/I^2$) calculations. Compliance of voltage and resistance noise spectra, which is in agreement with

Ohms law, is shown in **Figure 4a** and **b**. An increase of resistance noise due to high-voltage treatment is observed. Resistors based on compositions with higher sheet resistances exhibit smaller final change of the resistance noise. Since the same test conditions were applied to all test samples, the obtained results were expected. Results for all test resistors presented in **Table 1** show that measured resistance changes are less distinguished than the measured resistor noise spectrum changes.

High-voltage pulse stressing caused microscopic changes in thick resistive films that manifested in presented results. Thick resistive films are complex conductive networks. These conductive networks are result of the sintering processes. Transport of electrical charges takes place via a number of conducting chains. These chains consist of clusters of particles (particles that are in contact) and neighbouring particles separated by thin glass barriers (MIM units). Therefore, the current flow is being determined by metallic conduction through clusters of particles and tunnelling through glass barriers. Multiple tunnelling processes take place when the traps are present in glass barriers. Impurities introduced during technological processes and partial dissolution of metal-oxide in glass are responsible for the presence of traps. During high-voltage treatment, resistance change occurs due to barrier and contact resistance changes. High-voltage pulse stressing induces electrical field inside metal-insulator-metal unit that is not sufficient to induce dielectric breakthrough and therefore a decrease in the resistance due to the increase in a number of contacts between neighbouring particles does not occur. It is more likely that high-voltage treatment affects electrical charges captured within thin glass layers between neighbouring conducting particles or that the concentration of traps increases due to changes in microstructure of the resistor thus affecting noise performances of the resistor more than resistance values. Besides that, resistance decrease may occur due to the conversion of single chain from the non-conducting state to the conducting state. Under the same straining conditions, depending on the volume fraction of the conductive phase, thick-film resistor exhibits different changes in resistance values. A conductive/insulating phase ratio determines the microstructure of the thick resistive film and present conducting mechanisms as it is shown in scanning electron microscopy (SEM) micrographs of 10 and 100 kΩ/sq thick-film resistors given in **Figure 5**. It can be seen that resistors based on compositions with greater sheet resistances have greater content of the glass phase. For that reason the most of the neighbouring conducting particles are separated by thin glass barriers. In that case, the conducting mechanism known as multiple tunnelling becomes dominant. On the other hand, resistors based on compositions with lower sheet resistances have lower content of the glass phase and therefore large conductive areas are present. In that case, the conducting mechanism known as metallic conduction is also present. This also means that for the same voltage pulse, a greater electric field can be achieved within the thin glass layer between two neighbouring particles along with the greater current. For these reasons, resistors with smaller sheet resistances exhibit greater resistance changes caused by high-voltage treatment.

Measurements of the noise voltage spectrum showed that high-voltage treatment results in the increase of noise voltage and corresponding resistance noise spectra. Moreover, dominant contribution of the $1/f$ noise source is observed. High-voltage pulse stressing affects electrons captured by traps in thin glass barriers that are not directly involved in the conduction. However, conduction is being modulated by electrical charges captured by traps that alter the height of the potential barrier of metal-insulator-metal unit. For these reasons, change in the resistance noise

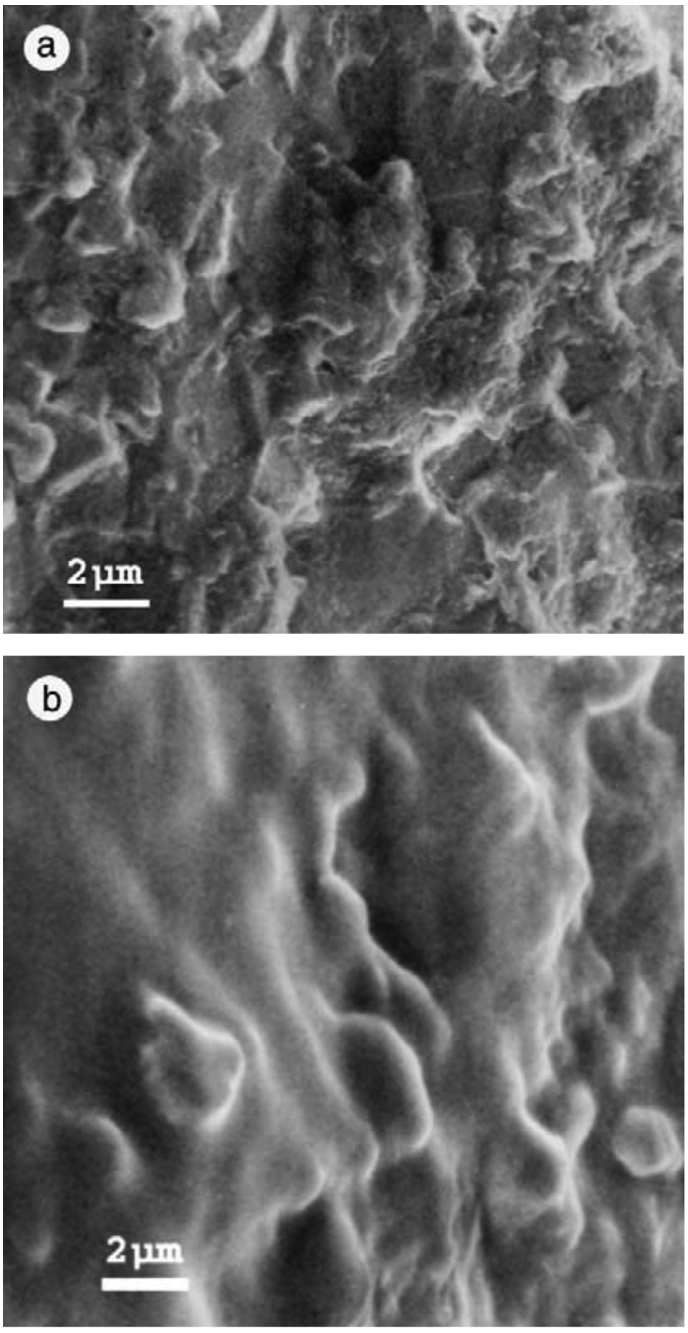

Figure 5. SEM micrographs of 10 kΩ/sq (a) and 100 kΩ/sq (b) thick-film resistors fired for 10 min at 850°C [12].

http://dx.doi.org/10.5772/intechopen.69442

spectrum is considerably higher than change in resistance values before and after high-voltage pulse stressing. It confirms the presumption that low-frequency noise exhibits greater sensitivity to changes at the microstructural level than resistance. Besides that, resistors formed using compositions with higher sheet resistances exhibit smaller resistance noise spectrum changes. Since it is noted that contacts between neighbouring conducting particles negligibly affect low-frequency noise, such behaviour can be attributed to differing spatial distributions of traps in resistors based on compositions with different sheet resistances. Along with measurements of noise voltage spectrum, noise index [15] measurements were performed since noise index is well known as one of the standard quality and reliability indicators used in the fabrication of thick resistive films. Noise index was measured before and after performed stressing. Measurements showed increasing noise index values due to applied stressing. As expected, the observed noise index increase is in agreement with the resistance noise spectrum measurements having in mind the noise index definition. However, noise spectra measurements can provide additional information regarding noise nature and sources that are related to microstructural properties of thick resistive films and present conducting mechanisms.

High-voltage treatment caused numerous catastrophic failures in tested resistors [12]. **Figure 6** shows failed 100 kΩ/sq thick-film resistor that was exposed to eleven 1500 V pulses and a single 3000 V pulse. A resistor with the initial resistance of $R = 111.92$ kΩ was covered with fine Ag powder that migrated from the contact area between resistive film and conducting path. Ag powder affected resistance of the resistor by decreasing its value. After the mechanical removal of the powder resistor regained its 100 kΩ value and damaged area became visible. As it can be seen from **Figure 6a**, the segregation of the resistive film took place. The cause of the failure is probably a faulty technological process that introduced impurities in the resistive film. The micrograph of the failure spot shown in **Figure 6b** showed that thin resistive layers still remained present in the failure region. The ratio between the glass and

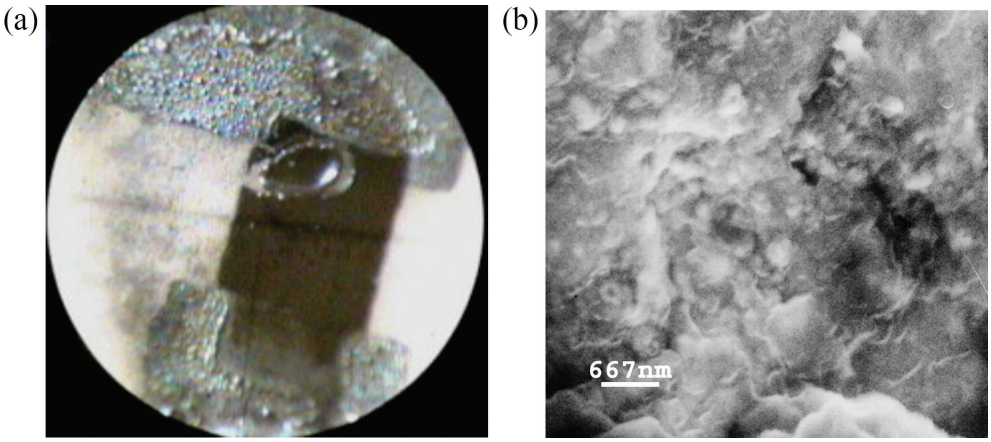

Figure 6. Photograph of 100 kΩ/sq thick-film resistor that catastrophically failed (a) and micrograph of the damaged area (b) [12].

conductive phase was changed because of the higher concentration of the conductive phase in the surface layer of the resistor. Several factors affected the performances of this resistor. High-voltage treatment affected both the microstructure and macrostructure of the resistor, introduced visible physical damage and damage caused by mechanical removal of thin layer of Ag powder.

In order to prove that high-voltage treatment caused microstructural changes in noise index and resistance noise spectra were measured. **Figure 7** and **Table 1** show that noise performances of the failed resistor were in correlation with noise performances of resistors that did not suffer failure. The segregated area accidentally did not strongly affect microstructure of the resistor. A thin conducting layer that remained at the failure spot probably had a shunting effect that compensated decreased thickness of the resistive film.

Figure 8a shows the failed 10 kΩ/sq thick-film resistor. The conducting film, as well as the contact area between resistive and conductive film, was damaged after the impact of a single 1500 V pulse. The possible cause of this occurrence may be defect migration or poorly formed contact between resistor and neighbouring conducting path. Resistance increase confirmed that the resistor area was affected. However, it cannot be concluded how this defect influenced the

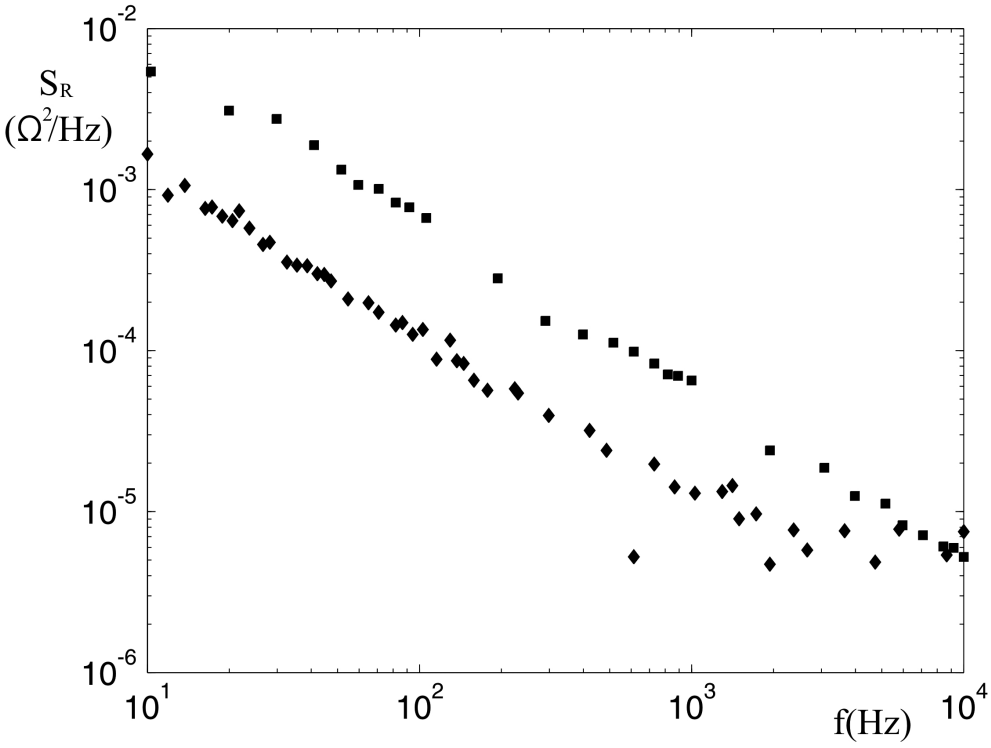

Figure 7. Experimental results for resistance noise spectrum (◆—before pulse stressing, ■—after pulse stressing) for catastrophically failed thick-film resistor with the initial resistance $R = 111.92$ kΩ [12].

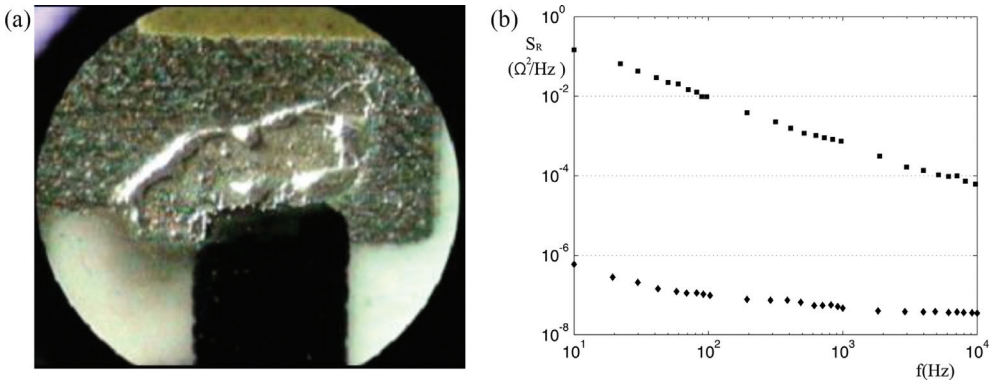

Figure 8. Photograph of catastrophically failed thick-film resistor (a) with the initial resistance $R = 7.842$ kΩ and experimental results for resistance noise spectrum (◆—before pulse stressing, ■—after pulse stressing) (b) [12].

frequency-dependent part of the low-frequency noise spectrum. According to the results given in previous figures, the resistance noise spectrum and noise index increases (**Figure 8b** and **Table 1**) are probably mainly related to changes in the microstructure of the resistive layer.

Figure 9 shows catastrophically failed resistor with a sheet resistance of 1 kΩ/sq [14]. Resistance of the thick-film resistor gradually increased with high-voltage pulse treatment until pulse amplitude reached its critical level at which resistor suffered catastrophic failure due to the excess loaded voltage. Both resistive film and conducting path were visibly damaged. As expected, pulse stressing also affected noise performances of the resistor. Noise index gradually increased with applied stressing until failures occurred resulting in maximal noise index values (**Figure 9a**). **Figure 9b** illustrates this mode of catastrophic failure.

During the high-voltage pulse treatment, destruction of the resistor may also occur. Conducting path degradation may lead to the dispersion of the conductive material to the resistor area resulting in the presence of local hot spots and resistor burning and evaporation. A typical example of this mode of catastrophic failure is shown in **Figure 10**.

During testing, several encapsulated resistors suffered progressive resistor degradation that led to catastrophic failure [13]. The photograph of the characteristic mode of progressive 10 kΩ/sq resistor degradation due to thermal effects induced by high-voltage treatment is given in **Figure 11**. Note that 10 kΩ/sq resistor was subjected to high-voltage pulse treatment using pulses with 3 and 4 kV amplitudes. With each applied 3 kV pulse resistor gradually degraded. At first, glass encapsulant started to melt and with further stressing several areas of thick resistive film became fully exposed to the environment. After increasing the pulse amplitude to 4 kV catastrophic failure took place. Thick resistive film burned and evaporated. The volume of the resistor decreased resulting in 430% resistance increase. The reported noise index values were in accordance with resistance values. Unacceptably high resistance and noise index values registering strain induced degradations along with diminished integrity of the resistive layer qualified this test resistor as unreliable.

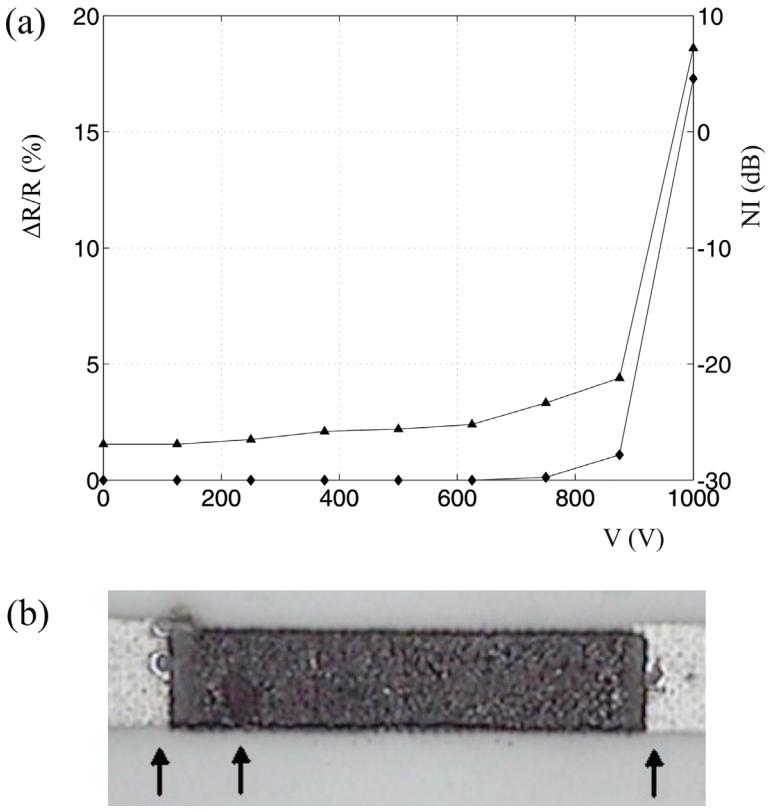

Figure 9. Experimental results for relative resistance changes and noise index during high-voltage pulse stressing of 1 kΩ/sq thick-film resistor (a) and a photograph of catastrophically failed resistor with designated failure points (b) [14].

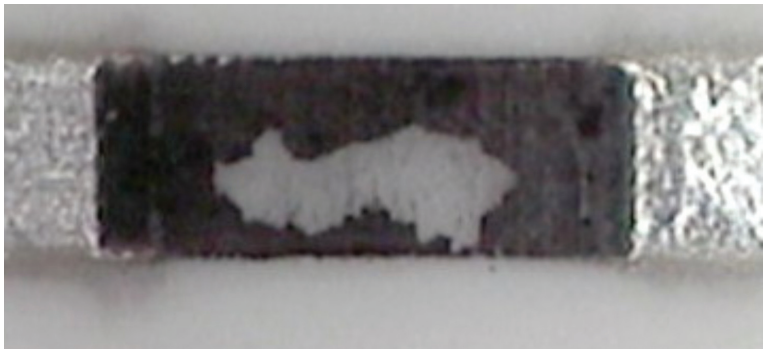

Figure 10. Photograph of catastrophically failed thick-film resistor due to the presence of hot spots caused by conducting material dispersion.

http://dx.doi.org/10.5772/intechopen.69442

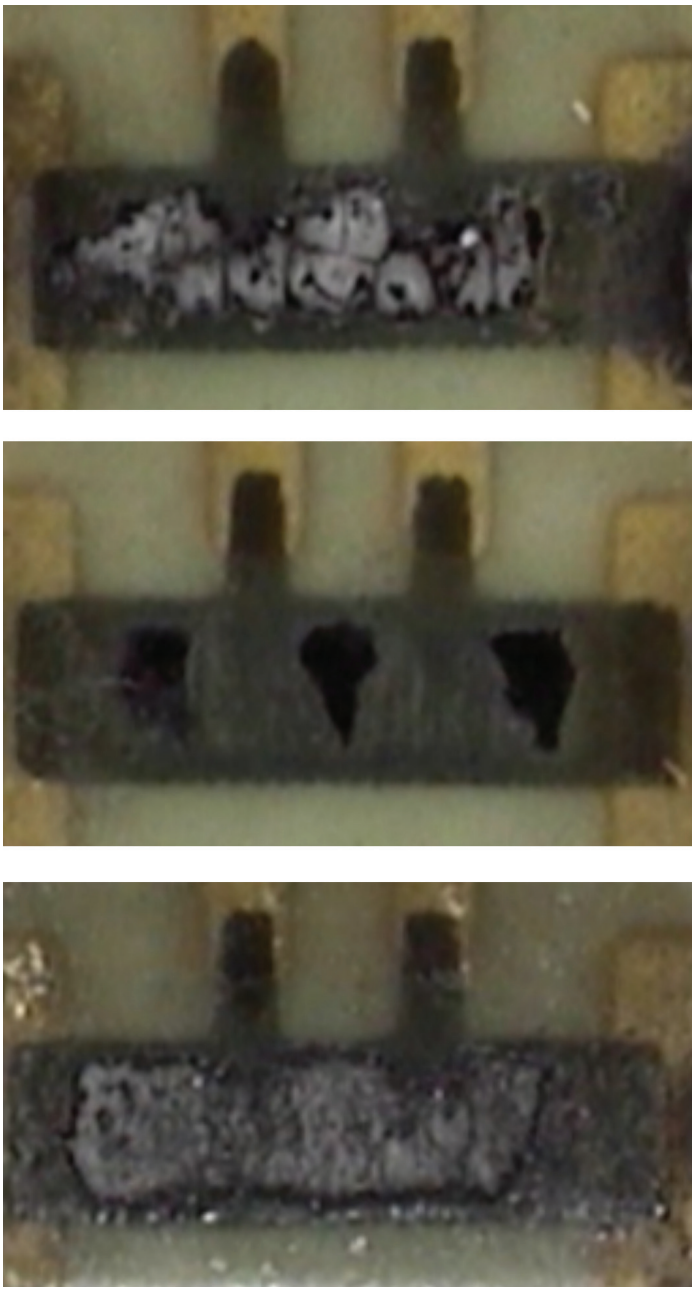

Figure 11. Photographs of progressive resistor degradation due to high-voltage pulse stressing: melting of glass encapsulant, direct exposure of resistive layer to surrounding atmosphere and burned and partially evaporated resistive layer [13].

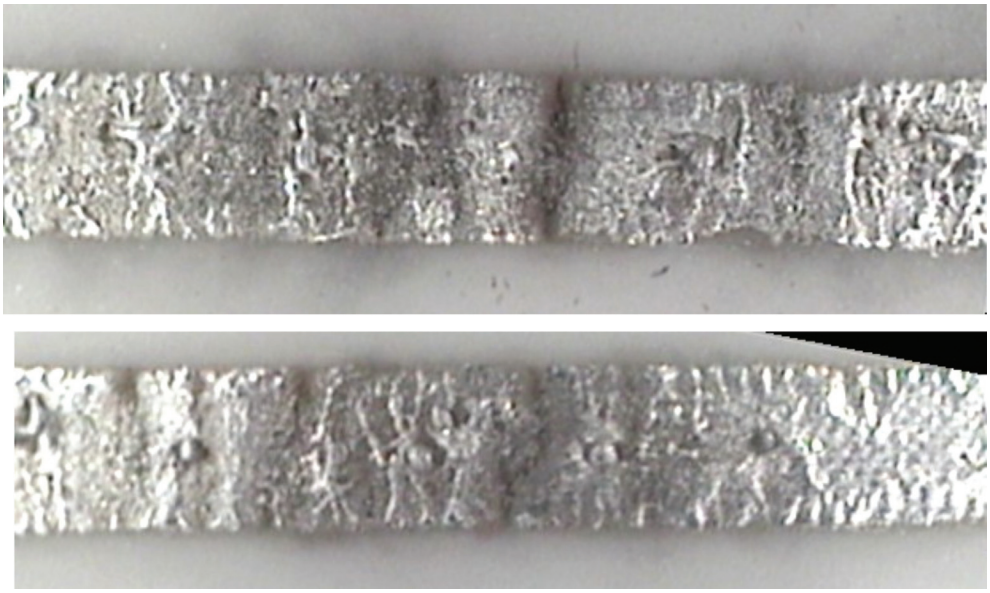

Figure 12. Photographs of failed conducting paths.

It should be mentioned that the failure of resistive layers due to high-voltage pulse stressing is often accompanied by the failure of conducting paths. The characteristics of failure modes for thick-film conducting paths are shown in **Figure 12**. The high-voltage treatment may diminish conducting path integrity causing burning and evaporation of conducting path segments.

4. Conclusion

Degradation and failure analysis of thick-film resistors is identified as the constant manufacturers challenge due to the growing market of C-MEMS devices and reliable communication systems. These contemporary applications of thick resistive materials induced the need to investigate their behaviour under various stressing conditions, especially electrical stressing conditions. On the other hand, there is a growing interest in noise measurements as means of thick-film resistor quality evaluation and evaluation of degradation under stress. For these reasons, this chapter presented the study of high-voltage pulse stressing effects on thick-film resistors based on the model of low-frequency noise in thick-film structures based on close relationship of the noise and conduction mechanisms. Correlation between resistance and low-frequency noise changes and high-voltage pulse stressing was observed and qualitative degradation and failure analysis was performed based on standard noise and resistance measurements. Several catastrophically failed resistors were presented and their failure modes were analysed. Results presented in this chapter confirmed that standard resistance and noise measurements can be used in degradation and failure analysis of thick resistive structures.

They aim to open new prospects for further investigations and quantitative analysis that may result in a method of diagnostic of microstructure effects as well as improved quality assessment of thick-film resistors under a wide range of extreme working conditions.

Acknowledgements

The authors would like to thank the Ministry of Education, Science and Technological Development of the Republic of Serbia for supporting this research within projects III44003 and III45007.

Author details

Ivanka Stanimirović

Address all correspondence to: inam@iritel.com

Institute for Telecommunications and Electronics IRITEL a.d. Beograd, Belgrade, Republic of Serbia

References

[1] Kusy A, Szpytma A. On 1/f noise in RuO_2-based thick resistive films. Solid-State Electronics. 1986;**29**:657-665. DOI: 10.1016/0038-1101(86)90148-6

[2] Chiang Y-M, Silverman LA, French RH, Cannon RM. Thin glass film between ultrafine conductor particles in thick-film resistors. The Journal of the American Ceramic Society. 1994;**77**:1143-1152. DOI: 10.1111/j.1151-2916.1994.tb05386.x

[3] Pike GE, Seager SH. Electrical properties and conduction mechanisms of Ru-based thick-film (cermet) resistors. Journal of Applied Physics. 1977;**48**:5152-5169. DOI: 10.1063/1.323595

[4] Hooge FN. 1/f noise is no surface effect. Physics Letters A. 1969;**29A**:139-140. DOI: 10.1016/0375-9601(69)90076-0

[5] Kleipenning TGM. On low-frequency noise in tunnel junctions. Solid-State Electronics. 1982;**25**:78-79. DOI: 10.1016/0038-1101(82)90100-9

[6] Mrak I, Jevtić MM, Stanimirović Z. Low-frequency noise in thick-film structures caused by traps in glass barriers. Microelectronics Reliability. 1998;**38**:1569-1576. DOI: 10.1016/S0026-2714(98)00032-8

[7] Jevtić MM, Stanimirović Z, Mrak I. Low-frequency noise in thick-film resistors due to two-step tunnelling process in insulator layer of elemental MIM cell. IEEE Transactions on Components, Packaging, and Manufacturing Technology. 1999;**22**(01):120-127. DOI: 10.1109/6144.759361

[8] Pellegrini B. 1/f $^{\gamma}$ noise from single-energy-level defects. Physical Review B. 1987;**35**(2): 571-580. DOI: 10.1103/PhysRevB.35.571

[9] Ehrhardt W, Thrust H. Trimming of thick-film-resistors by energy of high voltage pulses and its influence on microstructure. In: Proceedings of 13th European Microelectronics and Packaging Conference, May 31st–June 1st, Strasbourg, France, 2001; 403-407

[10] Dziedzic A, Kolek A, Ehrhardt W, Thust H: Advanced electrical and stability characterization of untrimmed and variously trimmed thick-film and LTCC resistors. Microelectronics Reliability. 2006;**46**:352-359. DOI:10.1016/j.microrel.2004.12.014

[11] Barker MF. Low Ohm resistor series for optimum performance in high voltage surge applications. Microelectronics International. 1997;**43**:22-26. DOI: 10.1108/13565369710800493

[12] Stanimirović I, Jevtić MM, Stanimirović Z. High-voltage pulse stressing of thick-film resistors and noise. Microelectronics Reliability. 2003;**43**:905-911. DOI: 10.1016/S0026-2714(03)00094-5

[13] Stanimirović I, Jevtić MM, Stanimirović Z. Multiple high-voltage pulse stressing of conventional thick-film resistors. Microelectronics Reliability. 2007;**47**:2242-2248. DOI: 10.1016/j.microrel.2006.11.017

[14] Stanimirović Z, Jevtić MM, Stanimirović I. Simultaneous mechanical and electrical straining of conventional thick-film resistors. Microelectronics Reliability. 2008;**48**:59-67. DOI:10.1016/j.microrel.2006.09.039

[15] Jevtić MM, Stanimirović Z, Stanimirović I. Evaluation of thick-film resistor structural parameters based on noise index measurements. Microelectronics Reliability. 2001;**41**:59-66. DOI: 10.1016/S0026-2714(00)00207-9